High Velocity Impact Tests on High Temperature Carbon-Carbon Composites

W.H. Xie [a], S.H. Meng [a,*], L. Ding [b], H. Jin [a], G.K. Han [a], L.B. Wang [a], Fabrizio Scarpa [c], R.Q. Chi [d]

[a] Center for Composite Materials and Structures, Harbin Institute of Technology, No.2 Yikuang Street, Harbin 150080, China

[b] Center for Advanced Composite Materials, Shenzhen Academy of Aerospace, Keji South Ten Road 6, Shenzhen, 518057, China

[c] Advanced Composites Centre for Innovation and Science (ACCIS), University of Bristol, BS8 1TR Bristol, UK

[d] Hypervelocity Impact Research Center, Harbin Institute of Technology, No.2Yikuang Street, Harbin 150080, China

Abstract

This paper describes the effect of high velocity impact on the structural integrity of advanced carbon-carbon (C/C) composites for high temperature applications. Impact tests have been performed on heated C/C composite samples at high temperature to establish correlations between the mechanical performances of the composites and different impact factors. Two tensile tests were also performed to investigate the residual strength of the high temperature C/C structures with the impact damage. In this work we present two new equations to predict the dimensionless damage areas of the C/C impacted at elevated temperatures. The impact resistance of the C/C composites is affected by the diameter of the projectile, the temperature and thickness of the C/C laminates and - more importantly – by the impact velocity. The residual strength of the damaged C/C composites increased by 47% after heating the samples from 25°C to 1206°C.

Keywords:

Carbon-carbon(C/C) composites; Impact behavior; High-temperature properties; Residual strength;

---

* This paper was presented at CCCM-2 held on Sept. 2015 in Zhenjiang, China.
Corresponding author: S.H. Meng, Email: mengsh@hit.edu.cn

Failure;

Nomenclature

Parameter	Definition
t_w	Laminate thickness
d_p	Diameter of the projectile
T	Temperature of the composite sample during the impact test
v_0	Impact velocity [km/s]
A_{front}	Area of the damage hole at the frontal side of the composite sample plate
A_{back}	Area of the damage hole at the back side of the composite sample plate
A_{front}/d_p^2	Dimensionless frontal damage area
A_{back}/d_p^2	Dimensionless back damage area

1. Introduction

Carbon-carbon composites are materials constituted by a carbon matrix reinforced with carbon fibers. Carbon-carbon composites are classified as reinforced carbon-carbon (RCC) and advanced carbon-carbon (ACC or C/C as abbreviation), and offer an unusual combination of thermal and mechanical properties [1-3]. RCC composites are essentially constituted by rayon fibers in carbon matrix, and the more recent ACC (based on PAN-based carbon reinforcements) are gradually replacing RCC structures. Due to their lightweight characteristics and high-temperature strength, general C/C are suitable candidate materials to satisfy the very stringent design requirements of reusable space vehicles and have been used as thermal protection systems (TPS) in airframes subjected to high temperature in hypersonic and reusable launch vehicles like the Space Shuttle[4, 5] Although the mechanical and

thermal properties of C/C composites are nowadays fairly well understood [6-8] and extensive investigations have been performed about the dynamic mechanical properties of "conventional" types of composites (i.e., resin matrix composites) [9-19], the knowledge about the high-speed impact dynamic behavior of C/C composites is still incomplete. Several research groups have studied the effect of the temperature on the dynamic properties and the impact damage at low temperature [20-23] and cryogenic environment [24, 25], but the temperature range usually limited between -150°C and 150°C due to the partial heat resistance capability of common composite materials. On the opposite, the environment in which hypersonic or reusable launch vehicles operate provides a large spectrum of potential threats to the structural integrity of the structures, with varying impact speeds. Orbital debris can hit spacecraft at velocities between 1 km/s to over 16 km/s[26]. With the sustained development of space activities and manned space flight during the last decades, the environment around the Earth has seen a significant concentration of the density of orbital debris that constitutes a remarkable threat to the safety of on-orbit space vehicles. It is therefore necessary to investigate the effect of the impact damage on the operational life and overall structural performance of carbon-carbon structures used in these spacecraft designs. Experimental and computational methods have been developed to acquire a better understanding of the impact response in carbon-carbon materials [27-33], although many existing results available in open literature are referred to RCC materials only. Christiansen et al. [34-36] have performed a series of hypervelocity impact tests on RCCs to determine their impact damage characteristics, establish damage threshold levels, and develop correlations to predict the impact damage. Curry et al. [37, 38] have presented experimental results obtained on RCC samples impacted by aluminum projectiles at velocities varying from 6.46 km/s to 7.12 km/s. In the same paper the authors have presented results related to arc jet tests to establish the oxidation characteristics of

RCCs at temperatures oscillating between 2500°F and 2800°F (1371°C – 1538 °C).

Impact test results for C/C in open literature are limited because of the costs involved in both the development and test of these composites, and confidentiality/intellectual property issues. Data related to high-velocity impact tests on C/C at elevated temperatures are also scarce [39-41]. This paper presents an experimental and analytical investigation on the effects of high velocity impact (1600 ms^{-1} – 4600 ms^{-1}) and related damage on C/C composites at high temperatures (between 25 °C and 1429 °C) using a fast electric heating system. Two series of tensile tests were also conducted to investigate the residual strength present in the C/C composites. The high-speed impact tests at high-temperature have been performed using a custom-made facility, and its design will be described in detail. The data obtained from the test campaign have been used to develop semiempirical equations that relate the dimensionless area damage of the composites with the temperature, impact speed and dimensions of the laminates.

2. Design of the high-temperature impact facility and test procedure

Fig.1 and Fig.2 show the two-stage light gas gun and the impact chamber with a fast electric heating system associated to the gas gun itself. The two-stage light-gas gun is used to accelerate the spherical projectiles, The fast electric heating system mainly consists of two copper (Cu) electrodes, a cooling water tank and a voltage transformer, and can be used to both heat the C/C composite samples and measure the temperature of the composites samples. The shape and size of the composite specimens shown in Fig.3 (a) are designed according to the dimensions constraints provided by the facilities. During each test the composite sample is clamped between the two Cu electrodes, which are fixed to a supporting back plate (Fig.1 (b)). To facilitate the insertion of the Cu electrodes the four corners of the samples were cut. The temperature of the composite specimen can be controlled through

a variable current with adjustable range (10A ~5000A). The voltage at the two ends of the composite sample was maintained at 1 V~ 4 V and the current amplitude controlled through a proprietary software. The temperatures of the composite samples were measured using two 2-colour pyrometers (IMPAC IGAR 12-LO MB10 (300 ºC~1000 ºC) and IMPAC ISR 12-LO MB33 (1000 ºC~3300 ºC), LumaSense Technologies, Inc. USA) with a measurement range between 300ºC to 3300ºC. The pressure in the chamber is maintained between 500 Pa and 800 Pa. A PHOTRON FASTCAM SA5 (USA) high-speed camera (256x256 pixels at 87500 fps, 128x128 pixels at 262500 fps) was used to capture time-resolved images of the travelling projectiles before impact. The sampling frequency of the images was adjusted according the impact velocity (around 90000 ～160000 frame per second (fps)). The distance between two positions of the projectile in the images at two distinct moments was divided by the time interval to calculate the impact velocity.

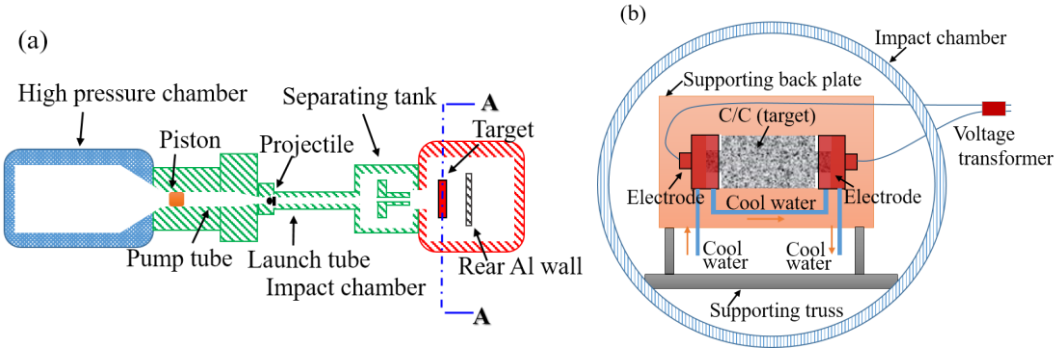

Fig.1. Schematics of the impact rig: (a) Two-stage light gas gun; (b) Setup of the impact chamber

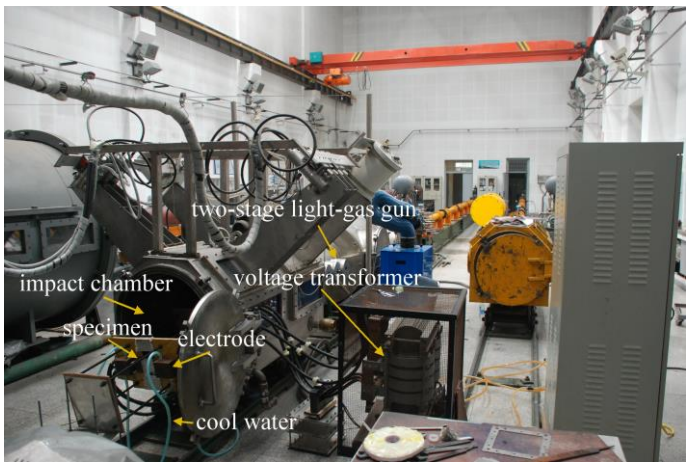

Fig.2 .Impact test setup

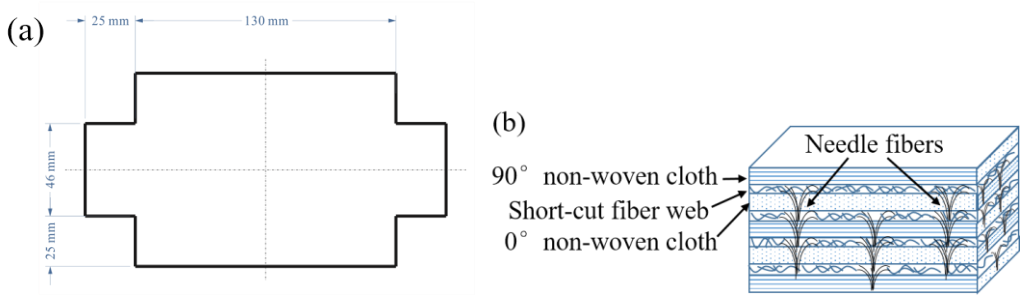

Fig.3.Sketch of C/C composite samples: (a) Dimension of composite sample; (b) Architecture of the needled preforms

The impact experiments were performed on 3 mm, 5 mm and 10 mm thick C/C composite samples. The C/C composite specimens used in this study consist in a needle-punched C/C composite. The C/C composite samples were made by hot isostatic pressure impregnation carbonization (HIPIC) based on the needled fiber preform. The carbon fiber was PAN-based carbon (T700, 12 K, Toray, Japan). The needled preform (Fig.3 (b)) were prepared using the three-dimensional needling technique, starting with repeatedly overlapping the layers of 0° non-woven fiber cloth, short-cut fiber web, and 90° non-woven fiber cloth by needle-punching at every step. The preform was then densified under a pressure of 80MPa ~100MPa followed by high temperature treatments (HTTs) at around 2500 ºC. These processes were carried out slowly (over 1-3 days) to obtain a high quality finish of the composites and guarantee a general excellent thermo-mechanical performance. The final C/C composite had a fiber volume fraction of ~20%, the volume fraction of the z-pin is ~1%, and a bulk density of around 1.97 g/cm^3. Spherical projectiles made of ZrO_2 and Si_3N_4 with diameters ranging from 1mm to 5mm impacted the C/C composite samples. The two different types of impactors have been used to compare the influence of the materials properties on the impact resistance of the C/C plates. Moreover, ZrO_2 and Si_3N_4 were selected as projectile materials because of their outstanding

hardness and toughness. Two composite specimens after tests were cut according to the ASTM Standard D 5766/D 5766M -02a for open hole tensile tests to investigate the residual strength after impacts.

3. Results and Discussion

3.1. Impact Test Results

Seventeen (17) high velocity impact tests have been performed. After the impact tests, damage was inspected on the front and back surfaces of the composite samples. The damage was quantified by measuring the areas of the perforated holes on the front and back surfaces. The damage areas were measured using an image processing analysis software ImageJ (Version 1.50b, National Institutes of Health, USA). Table 1 presents a summary of the impact test results and dimensionless damage areas. The C/C composite sample related to test #5 was not heated. The C/C composite sample belonging to test #1 was heated to approximately 1200°C for seven times and then it was impacted at 1205°C. The other composite samples were heated to the specified composite samples indicated in Table 1 by adjusting the output current amplitude with the pyrometers and the temperature control software, and then impacted. The heating rate varied between 10°C/s~200°C/s.

The results shown in Table 1 indicate that that the back surface of the perforated C/C composites features larger dimensionless damage areas compared the ones present in the front surface.

Table 1 Impact test results

NO.	Projectile material	T (°C)	v_0 (km/s)	Test result*	t_w/d_p	A_{front}/d_p^2	A_{back}/d_p^2	Impact energy(J)
1	Si_3N_4	1205	1.690	Perf	1.667	3.537	4.207	69.449
2	Si_3N_4	1206	1.680	Perf	1.667	1.781	2.498	68.629
3	Si_3N_4	1225	1.710	Perf	2.5	1.268	2.198	21.067
4	Si_3N_4	1230	1.700	No Perf	5	2.95	0	2.603
5	Si_3N_4	25	1.690	Perf	1.667	3.501	5.519	69.449
6	Si_3N_4	1212	1.980	Perf	1	3.100	3.225	441.334
7	Si_3N_4	1218	1.676	No Perf	3	3.42	0	2.530

8	Si_3N_4	1270	2.000	No Perf	5	3.82	0	3.602
9	Si_3N_4	1230	1.704	Perf	1	3.376	3.999	326.871
10	ZrO_2	1193	1.760	Perf	1.667	2.928	3.799	131.374
11	Si_3N_4	1205	1.700	Perf	1	2.640	3.303	70.273
12	Si_3N_4	900	1.700	Perf	3.333	2.090	3.591	70.273
13	Si_3N_4	819	1.886	Perf	1.667	8.998	10.956	86.492
14	Si_3N_4	1429	1.608	Perf	1.667	4.143	10.754	62.873
15	Si_3N_4	1220	4.600	Perf	1.667	21.32	25.169	514.525
16	Si_3N_4	1205	3.090	Perf	1.667	11.133	11.364	232.171
17	Si_3N_4	1234	3.900	Perf	5	12.554	14.52	13.698

*Perf: the C/C composite sample was perforated; No Perf: the C/C composite sample was not perforated.

Fig.4 shows some examples of the impact damage states on the front and back surfaces of the C/C composites tested at room temperature (test #5). Fig.5 is related to test #2 and shows two representative photographs of the damage on the composite at 1206ºC. It is possible to observe that at that temperature the texture of the surface of the ACC composite shows more clearly the structure of the non-woven cloth. Apart from test #1, the mass loss corresponding to each test was observed to be negligible. The projectiles used in tests #8 and #10 were shattered after impacting the composites composite samples, but the ones of the other tests were not significantly damaged. No phase transition [42] of the projectile materials was observed during all the tests.

From open literature one can observe the appearance of three distinct regimes occurring during the impacts of composites specimens. The first is typical of small impact velocities, with the perforation being dominated by the petalling of the rear surface plies. In the second the perforation mechanism of the composites changes from one dominated by petalling to another characterized by a conically shaped plug formation. The residual velocity rapidly reduces with the increasing velocity of the projectile. The third regime is characterized by the perforation mechanism of composites being dominated by shaped plug formation, causing no plug but compression/shear failure in the target [43].

All samples showed the presence of a clear penetration channel, and the perforation mechanism of the C/C composite samples at high temperatures appeared to be dominated by shaped plug formation, which is the third regime mentioned above. No plug was present, instead a compression/shear failure could be observed. The shapes of the passing holes are all similar and tend to assume a square topology. Fibers of the front and back surfaces were pull out, which is a characteristic of tensile type of failure[43]. The carbon matrix is brittle, and consequently brittle failure had occurred during the penetration of the projectiles.

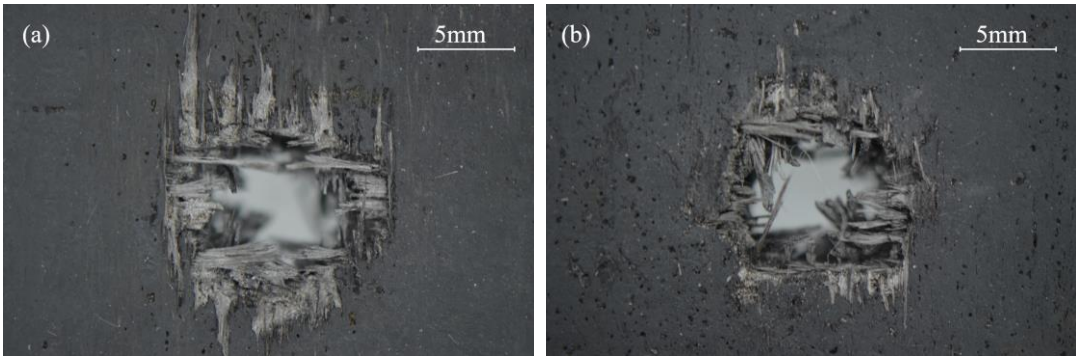

Fig.4.Impact damage on the front and back surface of test #5: (a) Front surface; (b) Back surface

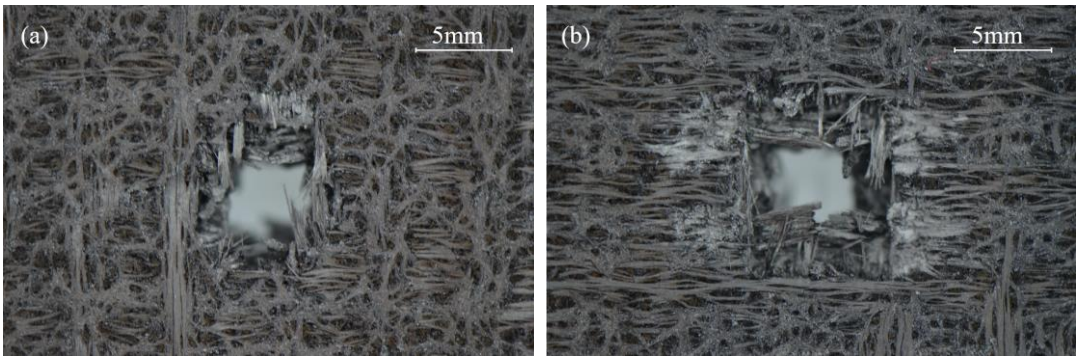

Fig.5.Impact damage on the front and back surface of test #2: (a) Front surface; (b) Back surface

3.2. Effects of the different impact factors

3.2.1. Oxidation times

To investigate the effect of the oxidation times, the C/C composite sample used during test #1 was heated to approximately 1200°C for seven times before the impact. The C/C composite sample was

then impacted by a 3mm-diameter Si_3N_4 projectile at a temperature of 1205°C., The composite sample lost weight after every heating cause the oxidization of the matrix material. The differences between the impact temperatures of tests #1 and #2 were around 1°C. The differences between the impact velocities of tests #1 and #2 were 10 m/s, with all the other conditions being the same. The impact damage of the C/C composite specimen in test #1 was larger than the one of test #2, indicating that the longer the oxidation times the poorer the resistance to the perforation becomes. The influence of the mass loss of the C/C should be considered when taking into account multi-oxidation impacts.

3.2.2. Composite sample thickness and projectile diameters

Fig.6 illustrates the dimensionless damage area as a function of the ratio t_w/d_p . The differences between the impact temperatures of tests #2 and #11 were around 1°C, while the impact velocities were differing of 20 m/s. Also in this case all the other impact conditions of tests #2 and #11 were the same. The results from these results indicate that by increasing the thicknesses of the composite specimens from 3mm to 5mm the perforated hole-areas of the front and back surfaces decrease.

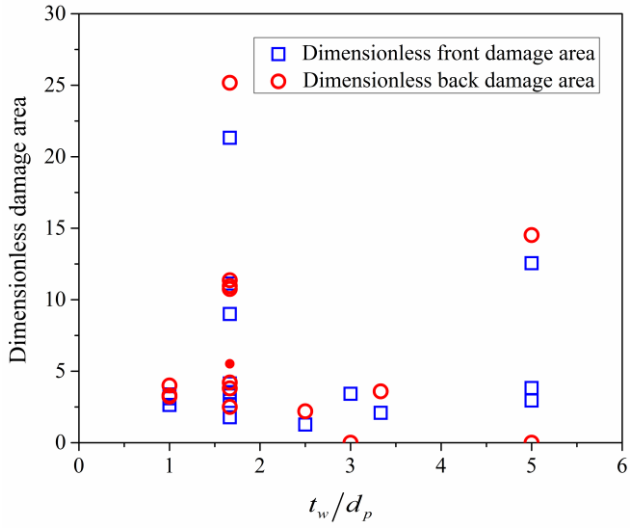

Fig.6.Dimensionless damage area as a function of t_w/d_p

3.2.3. Impact temperature

Fig.7 illustrates the dimensionless damage area as a function of the impact temperature. The

impact temperature of test #2 was 1181°C higher than the one of test #5, while the impact velocities of these two tests were very close to each other (differing only by10 m/s) and the other impact conditions were equal. The damages of the front and back surfaces of the composite sample from test #2 were smaller than those corresponding to test #5, and this indicates that the resistance to impact of the C/C composite specimen increased after heating. After being impacted by the projectiles, the perforated composite samples of tests #2 and #5 were cut to investigate the residual strength by tensile tests. The specimens of the tensile tests with the holes generated by projectile impacts are shown in Fig.8. The tensile test showed that the residual strength corresponding to test #2 was 47% higher than the one identified from loading the composite sample of test #5, i.e. the residual strength of the C/C composite samples could be increased through heating.

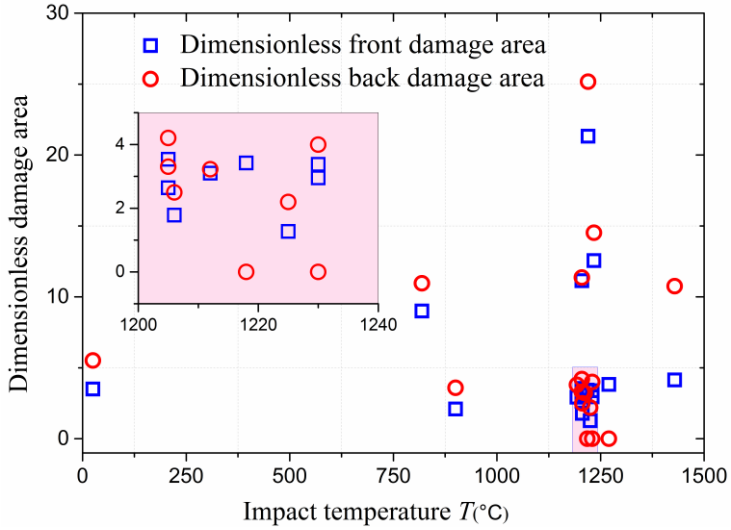

Fig.7.Dimensionless damage area as a function of the impact temperature

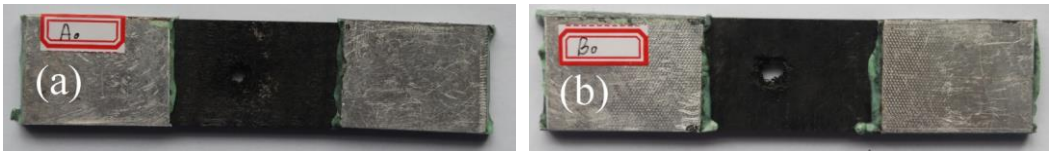

Fig.8.Tensile test specimen corresponding to impact tests (a) #2 and (b) #5 after test

3.2.4. Projectile materials

The composite samples corresponding to tests #2 and #10 were both perforated by the

3mm-diameter projectiles made from Si_3N_4 and ZrO_2. The hole of the front and back surfaces of the composite sample in test #2 had a smaller surface than the one in the sample #10. A backing aluminum wall was placed behind the specimens during tests #2 and #10. The damage states of the rear walls of both tests are shown in Fig.9. The rear aluminum wall was perforated in test #10, but not perforated during test #2. Since the projectile of test #10 was shattered after perforating the C/C composite sample and the impact velocity and temperature were different, it is difficult to ascertain the perforation abilities of the ZrO_2 and Si_3N_4 projectiles by these only two test results.

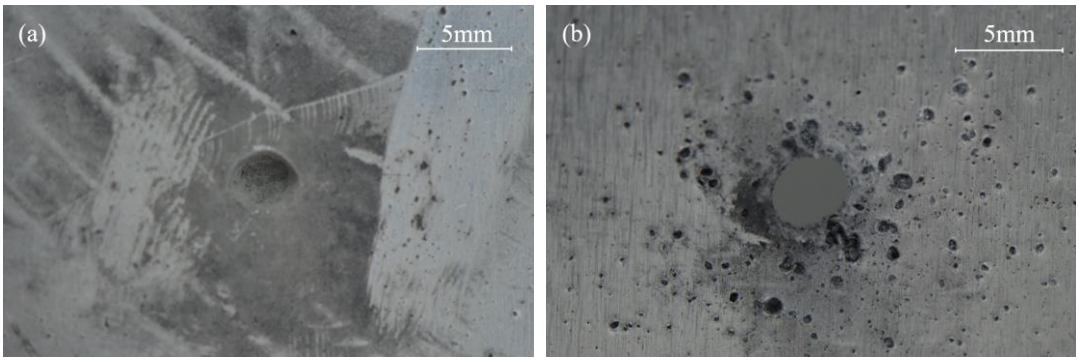

Fig.9.Impact damage states on the rear aluminum wall for tests #2 and #10: (a) #2 Si_3N_4 and (b) #10 ZrO_2 projectiles

3.2.5. Impact velocity

Fig.10 illustrates the dimensionless damage area of the composites as a function of the impact velocity.

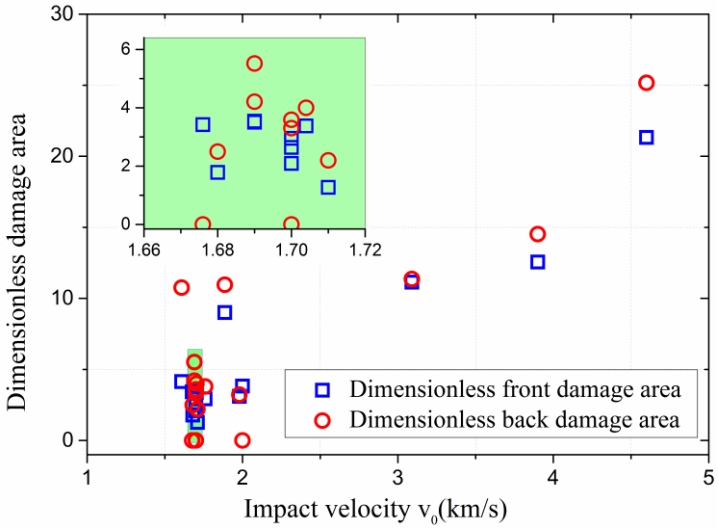

Fig.10.Dimensionless damage area as a function of the impact velocity

Previous hypervelocity impact tests had been conducted to establish the damage modes on coated C/C composites at room temperature. Christiansen *et al* have developed equations to predict the hole's diameter D_h when a complete penetration of reinforced carbon composites (RCC) occurs [34-36].

The form of D_h is shown in Eq. (1) [36]:

$$D_h = 2.20 d_p \rho_p^{1/3} \left(v_0 \cos\theta\right)^{1/3} - 0.36 \tag{1}$$

In Eq. (1), ρ_p is the projectile density and θ is the impact angle from surface normal.

We have developed two new sets of equations for the C/C composites to predict the dimensionless damage areas $A_{front}/d_p^{\,2}$ and $A_{back}/d_p^{\,2}$:

$$A_{front}/d_p^{\,2} = 11.090\left(T/\mathrm{T}_0\right)^{-0.027}\left(v_0/\mathrm{c}_t\right)^{1.175}\left(t_w/d_p\right)^{-0.150} \text{-}4.925 \qquad [\mathrm{R}^2=0.998] \tag{2}$$

$$A_{back}/d_p^{\,2} = 11.219\left(T/\mathrm{T}_0\right)^{-0.117}\left(v_0/\mathrm{c}_t\right)^{1.655}\left(t_w/d_p\right)^{-0.223} \text{-}2.068 \qquad [\mathrm{R}^2=0.944] \tag{3}$$

In the two presented equations, T_0=25°C is the room temperature, c_t =1.91km/s is the speed of sound in carbon/carbon composites [44].

Fig.11 and Fig.12 show the comparisons between the experimental results and the predictions from Eq. (2) and Eq. (3), respectively. The predicted values of A_{front}/d_p^2 from Eq. (2) were significantly lower (> 55%) than the experimental data in one case, and in two when the dimensionless parameter

A_{back}/d_p^2 was considered. For all the other cases, the predicted values were conservative compared to the experimental results, with the largest discrepancies at ~ 38% in five cases. Overall, within the population of 17 test data, Equations (2) and (3) appear to provide adequately robust predictions.

While a population of 17 results may be not large in absolute sense, its dimension is compatible with the one presented in other relevant works published in open literature. For example, Corbett uses a total number of tests equating 21 for his regression analysis, with fourteen of them related to high temperature tests[45] (and not the sixteen used in this work). The equations capture in any case the essential features that the damage of the C/C increases with the impact velocity and the projectile diameter, and decreases with the impact temperature and the thickness of C/C, which agreed with the test results. Moreover, by comparing the power exponents of the ratios T/T_0, $v_0/\mathrm{c}_\mathrm{t}$ and t_w/d_p it is possible to notice that the impact velocity might be more important for the impact damage of the heated C/C composites. Lastly, the effects of the impact velocity and temperature for the damage of the back surface of C/C composite sample might be more significant than in the case of the front surface.

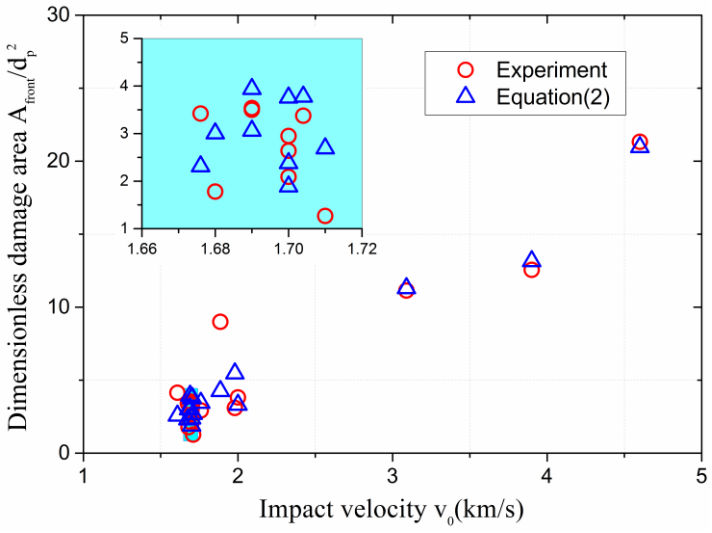

Fig.11.Comparisons of experimental results and predictions of A_{front}/d_p^2

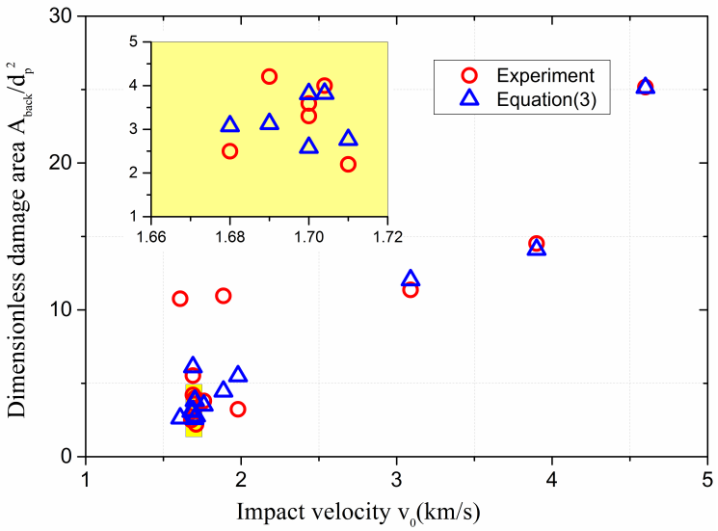

Fig.12.Comparisons of the experimental results and predictions of A_{back}/d_p^2

Fig.13 shows the comparison between the experimental and different analytical predictions of the dimensionless damage area A_{hole}/d_p^2 calculated as follows:

$$A_{hole}/d_p^2 = \left(\pi D_h^2/4\right)/d_p^2 \tag{4}$$

Where D_h is the hole size calculated by Eq. (1) with θ =0. To represent the various points within a single family of curves, Figures 13(a) and 13(d) have the curves from Equations (2) and (3) and from Reference [24] drawn at average temperatures of 1206ºC and 1245ºC, respectively. The difference between these temperatures and the maximum temperature of the samples during test is 27ºC and 41ºC for the two cases. Equations (2) and (3) show however a maximum difference of 40ºC in terms of sensitivity versus the temperature, therefore the two regressions presented in this paper provide very similar behaviors within the temperature interval considered.

The curves presented in Equations (2) and (3) follow a similar general trend to the one shown by Christiansen and Friesen [36], although with some differences. At room temperature (Fig.13b), Christiansen & Friesen's prediction is lower than the one provided by the equations described in this paper at impact velocities larger than about 2.5km/s. For all the other cases, the differences between our predictions and the curve from [36] is quite large. Christiansen and Friesen's equation

is mainly based on hypervelocity impact tests (at more than 6km/s) and it quantifies the impact damage by one single parameter (the size of the hole after perforation), not considering the influence of the temperature during impact. While the test results at room temperature seem to be sufficiently well represented by the equations developed in this paper and in [24] (Fig. 13b), the equation from reference [36] tends to predict in a less adequate manner the damage size at high temperatures for impact velocities lower than ~ 5 km/s (Figs. 13a, 13c and 13d). Fig.11-Fig.13 globally show that the equations derived in this paper give general good agreements with most of the experimental results at different impact temperatures, velocities, materials and ratios of composite sample thickness to projectile diameter.

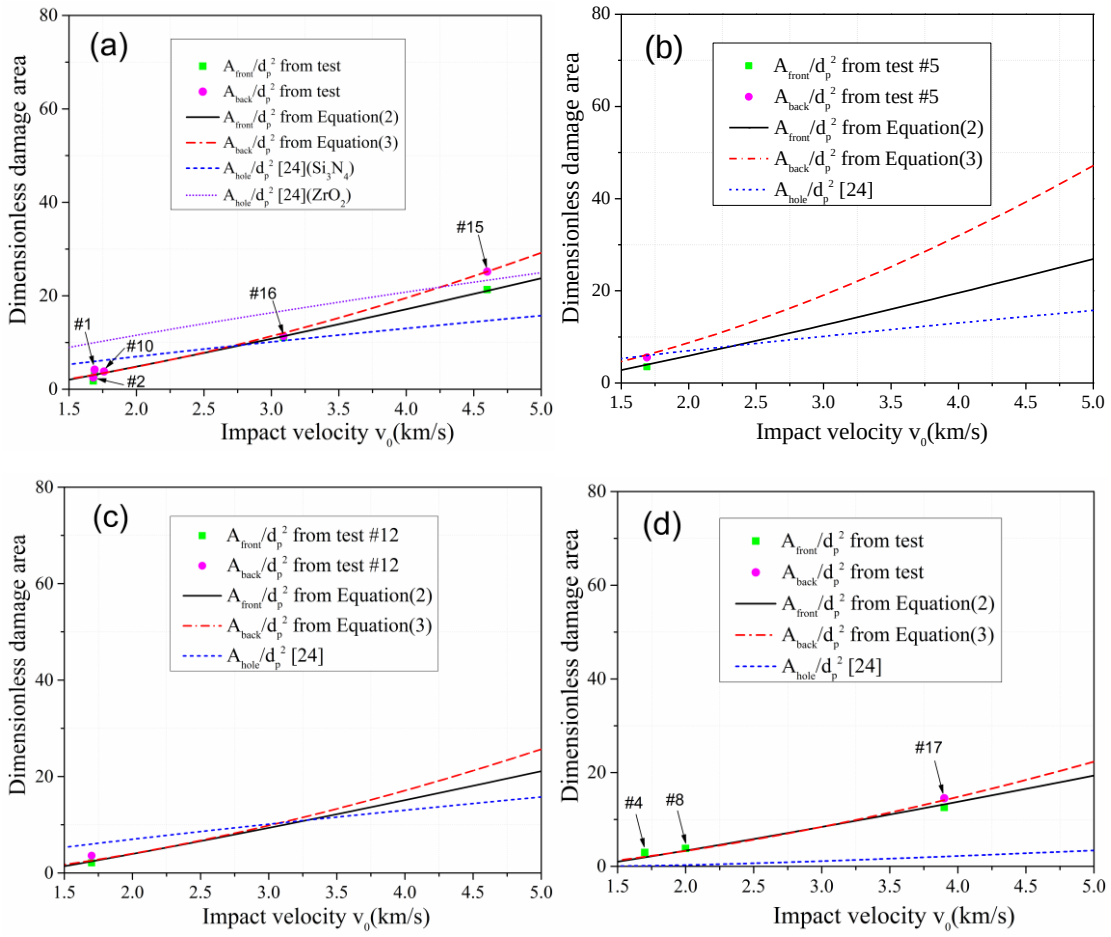

Fig.13. Comparisons between tests data and prediction equations related to samples (a) #1, #2, #10, #15, #16; (b) #5; (c) #12; (d) #4, #8, #17. The detailed test conditions are given in Table 1.

4. Conclusions

This paper has presented a series of experimental results related to high velocity impacts at high temperature on C/C composite samples. The damage states on the front and back surfaces of the composite specimens were analyzed and quantified by determining dimensionless damage areas parameters. Two tensile tests were also performed to identify the residual strength. Two new prediction equations for the damage of the C/C composites were developed in this paper. From the results acquired in this paper it is possible to conclude the following:

1) The effect of the impact velocity on the impact resistance of C/C composites appears to be more important than the dimensions of the projectile diameter, the testing temperature and the thickness of the samples;
2) The impact resistance increases after a single heating ramp from 25°C to 1206°C. The corresponding residual strength after the impacts increased by 47%.
3) The predictive equations presented in this paper agree with the experimental results and also describe the effect of temperature by introducing terms depending on the temperature ratio normalized by room temperature.

Acknowledgements

This work has been supported by the Natural Science Foundation of China (11272107, 11472092 and 11502058) and the National Basic Research Program of China (973 program, No. 2015CB655200).

References

[1] Windhorst T, Blount G. Carbon-carbon composites: a summary of recent developments and applications. Mater Design 1997;18(1):11-5.

[2] Glass DE, Dirling R, Croop H, Fry TJ, Frank GJ. Materials development for hypersonic flight vehicles. 14th AIAA/AHI space planes and hypersonic systems and technologies conference, Canberra, AIAA2006.

[3] Tang Y, Zhou Z, Pan S, Xiong J, Guo Y. Mechanical property and failure mechanism of 3D Carbon–Carbon braided composites bolted joints under unidirectional tensile loading. Mater Design

2015;65:243-53.
[4] Haddad N, McWilliams H, Wagoner P. NASA Engineering Design Challenges: Thermal Protection Systems. EP-2008-09-122-MSFC. National Aeronautics and Space Administration (NASA) 2007.
[5] Savage E. Carbon-carbon composites: Springer Science & Business Media 2012.
[6] Buckley JD, Edie DD. Carbon-carbon materials and composites: William Andrew 1993.
[7] Ohlhorst CW, Vaughn WL, Ransone PO, Tsou H-T. Thermal conductivity database of various structural carbon-carbon composite materials: National Aeronautics and Space Administration, Langley Research Center 1997.
[8] Shigang A, Daining F, Rujie H, Yongmao P. Effect of manufacturing defects on mechanical properties and failure features of 3D orthogonal woven C/C composites. Composites Part B: Engineering 2015;71:113-21.
[9] Naik N, Ramasimha R, Arya H, Prabhu S, ShamaRao N. Impact response and damage tolerance characteristics of glass–carbon/epoxy hybrid composite plates. Composites Part B: Engineering 2001;32(7):565-74.
[10] López-Puente J, Zaera R, Navarro C. The effect of low temperatures on the intermediate and high velocity impact response of CFRPs. Composites Part B: Engineering 2002;33(8):559-66.
[11] Riedel W, Nahme H, White DM, Clegg RA. Hypervelocity impact damage prediction in composites: Part II—experimental investigations and simulations. Int J Impact Eng 2006;33(1):670-80.
[12] López-Puente J, Zaera R, Navarro C. Experimental and numerical analysis of normal and oblique ballistic impacts on thin carbon/epoxy woven laminates. Composites Part A: applied science and manufacturing 2008;39(2):374-87.
[13] Fernández-Fdz D, López-Puente J, Zaera R. Prediction of the behaviour of CFRPs against high-velocity impact of solids employing an artificial neural network methodology. Composites Part A: Applied Science and Manufacturing 2008;39(6):989-96.
[14] Muhi R, Najim F, De Moura M. The effect of hybridization on the GFRP behavior under high velocity impact. Composites Part B: Engineering 2009;40(8):798-803.
[15] Wang B, Wu L-Z, Ma L, Feng J-C. Low-velocity impact characteristics and residual tensile strength of carbon fiber composite lattice core sandwich structures. Composites Part B: Engineering 2011;42(4):891-7.
[16] Buitrago BL, García-Castillo SK, Barbero E. Influence of shear plugging in the energy absorbed by thin carbon-fibre laminates subjected to high-velocity impacts. Composites Part B: Engineering 2013;49:86-92.
[17] Pernas-Sánchez J, Artero-Guerrero J, Viñuela JZ, Varas D, López-Puente J. Numerical analysis of high velocity impacts on unidirectional laminates. Compos Struct 2014;107:629-34.
[18] Cherniaev A, Telichev I. Meso-scale modeling of hypervelocity impact damage in composite laminates. Composites Part B: Engineering 2015;74:95-103.
[19] Bandaru AK, Ahmad S. Numerical simulation of progressive damage in laminated composites under ballistic impact. Composites Part B: Engineering 2016.
[20] Jia Z, Yuan G, Ma H-l, Hui D, Lau K-t. Tensile properties of a polymer-based adhesive at low temperature with different strain rates. Composites Part B: Engineering 2016;87:227-32.
[21] Wosu S, Hui D, Daniel L. Hygrothermal effects on the dynamic compressive properties of graphite/epoxy composite material. Composites Part B: Engineering 2012;43(3):841-55.
[22] Im K-H, Cha C-S, Kim S-K, Yang I-Y. Effects of temperature on impact damages in CFRP composite laminates. Composites Part B: Engineering 2001;32(8):669-82.

[23] Suvarna R, Arumugam V, Bull D, Chambers A, Santulli C. Effect of temperature on low velocity impact damage and post-impact flexural strength of CFRP assessed using ultrasonic C-scan and micro-focus computed tomography. Composites Part B: Engineering 2014;66:58-64.
[24] Dutta PK, Hui D. Low-temperature and freeze-thaw durability of thick composites. Composites Part B: Engineering 1996;27(3):371-9.
[25] Ma H-l, Jia Z, Lau K-t, Leng J, Hui D. Impact Properties of Glass Fiber/Epoxy Composites at Cryogenic Environment. Composites Part B: Engineering 2016.
[26] Kessler DJ, Reynolds RC, Anz-Meador PD. Orbital debris environment for spacecraft designed to operate in low Earth orbit. DTIC Document 1989.
[27] Grujicic M, Pandurangan B, Zhao C, Biggers S, Morgan D. Hypervelocity impact resistance of reinforced carbon–carbon/carbon–foam thermal protection systems. Appl Surf Sci 2006;252(14):5035-50.
[28] Gwinn KW, Metzinger KE. Analysis of foam impact onto the Columbia shuttle wing leading edge panels using PRONTO3D/SPH. 42 nd AIAA Aerospace Sciences Meeting and Exhibit, Jan 5-8, 2004, Reno, NV2004. p. 2004-942.
[29] Humes DH. Hypervelocity impact tests on Space Shuttle Orbiter RCC thermal protection material. J Spacecraft Rockets 1978;15(4):250-1.
[30] Lu W-Y, Antoun B, Korellis J, Scheffel S, Lee M, Hardy R, et al. Material characterization of shuttle thermal protection system for impact analyses. J Spacecraft Rockets 2005;42(5):795-803.
[31] Park Y-K, Fahrenthold EP. Simulation of hypervelocity impact effects on reinforced carbon-carbon. J Spacecraft Rockets 2006;43(1):200-6.
[32] Wang S-X, Wu L-Z, Ma L. Low-velocity impact and residual tensile strength analysis to carbon fiber composite laminates. Mater Design 2010;31(1):118-25.
[33] Xu P, Zheng J, Liu P. Finite element analysis of burst pressure of composite hydrogen storage vessels. Mater Design 2009;30(7):2295-301.
[34] Christiansen EL, Ortega J. Hypervelocity impact testing of shuttle orbiter thermal protection system tiles. AIAA Paper 1990(90-3666):25-8.
[35] Christiansen EL, Curry DM, Kerr JH, Crews JH, Cykowski E, Crews JL. Evaluation of the Impact Resistance of Reinforced Carbon-Carbon. Proceedings of the ninth International Conference on Composite Materials (ICCM-9). Madrid Spain: Woodhead Publishing Limited 1993. p. 498-507.
[36] Christiansen EL, Friesen L. Penetration equations for thermal protection materials. Int J Impact Eng 1997;20(1):153-64.
[37] Curry DM, Center LBJS. Oxidation of Reinforced Carbon-carbon Subjected to Hypervelocity Impact: National Aeronautics and Space Administration, Lyndon B. Johnson Space Center 2000.
[38] Curry DM, Pham VT, Norman I, Chao DC. Oxidation of hypervelocity impacted reinforced carbon-carbon. J Spacecraft Rockets 2000;37(3):310-7.
[39] Fahrenthold EP. Computational Design of Orbital Debris Shielding.
[40] Kalinski ME. Hypervelocity Impact Analysis of International Space Station Whipple and Enhanced Stuffed Whipple Shields. DTIC Document 2004.
[41] Son KJ, Fahrenthold EP. Simulation of Orbital Debris Impact on Porous Ceramic Tiles. J Spacecraft Rockets 2014;51(4):1349-59.
[42] Hopkins A, Lee T, Swift H. Material phase transformation effects upon performance of spaced bumper systems. J Spacecraft Rockets 1972;9(5):342-5.
[43] Hazell P, Cowie A, Kister G, Stennett C, Cooper G. Penetration of a woven CFRP laminate by a high

velocity steel sphere impacting at velocities of up to 1875m/s. Int J Impact Eng 2009;36(9):1136-42.
[44] Fahrenthold EP, Park Y-K. Simulation of foam impact effects on components of the space shuttle thermal protection system. AIAA Paper 2004(2004-940):5-8.
[45] Corbett BM. Hypervelocity impact damage response and characterization of thin plate targets at elevated temperatures: ProQuest 2008.